Electronic Supplementary Information

Giant optical anisotropy of a highly stable metal-organic framework based on trinuclear iron(III) secondary building units linked by tetracarboxylic linkers with an anthracene core

A. V. Vinogradov,*[a] V. A. Milichko,[a] H. Zaake-Hertling,[b] A. Aleksovska,[b] S. Gruschinski,[b] S. Schmorl,[b] B. Kersting,[b] E. M. Zolnhofer,[c] J. Sutter,[c] K. Meyer,[c] P. Lönnecke[b] and E. Hey-Hawkins*[b]

a) ITMO University, St. Petersburg, 197101, Russian Federation.
b) Leipzig University, Faculty of Chemistry and Mineralogy, Institute of Inorganic Chemistry, D-04103 Leipzig, Germany.
c) Friedrich-Alexander University Erlangen - Nürnberg (FAU), Department of Chemistry & Pharmacy, Inorganic Chemistry, D-91058 Erlangen, Germany

1. General Methods and Instruments

2. Characterisation

3. X-Ray Powder Diffraction Studies of **1**

4. Surface Area of **1** and Pore Size Distribution

5. Additional Pores in Directions 011, 101, 110 and 111 of **1**

6. Magnetic Susceptibility of **1**

7. Mößbauer Spectroscopy of **1**

8. Thermal Properties (DTA/TG) of **1**

9. Optical Properties of **1**

10. X-ray Data for **1**

11. Ring Plane Angles in **1**

1. General Methods and Instruments

UV-Vis:
was carried out with a Perkin-Elmer Lambda 900 spectrometer.
Fluorescence was measured with a Perkin-Elmer LS50B.

DTA / TG:
Thermogravimetric analysis was carried out on a Netzsch STA/QMS STA 449F1 system in alumina crucibles. Helium (ca. 20-25 ml/min) was used as carrier/inert gas flow, creating an atmosphere that is close to normal pressure. The "combustion" chamber was evacuated and refilled with He twice. The He flow was continued for about 15-20 min before starting the measurements to allow equilibration of the system (buoyancy and decay of balance's oscillation). Alumina crucibles were used for the samples.

Powder diffraction:
X-ray powder patterns were obtained using a Bruker SMART Apex-II diffractometer operating with CuK_α radiation (λ_{Cu} = 1.54 Å). Analysis of structural data from powder diffraction was performed with the program package Platon.[1]

Magnetic susceptibility:
Magnetic data were collected using a Quantum Design MPMS-XL SQUID magnetometer. Measurements were obtained for a finely ground microcrystalline powder restrained within a polycarbonate gel capsule. DC susceptibility data were collected in the temperature range from 2 to 300 K under a DC field of 1 T. The data were corrected for core diamagnetism of the sample estimated using tabulated Pascal's constants.[2]

Mößbauer Spectroscopy:
^{57}Fe Mößbauer spectra were recorded on a WissEl Mößbauer spectrometer (MRG-500) at 77 K in constant acceleration mode. ^{57}Co/Rh was used as the radiation source. WinNormos for Igor Pro software has been used for the quantitative evaluation of the spectral parameters (least-squares fitting to Lorentzian peaks). The minimum experimental line widths were 0.20 mms^{-1}. The temperature of the samples was controlled by an MBBC-HE0106 MÖSSBAUER He/N_2 cryostat within an accuracy of ±0.3 K. Isomer shifts were determined relative to α-iron at 298 K.

EPR measurements:
EPR measurements were performed in air-tight J. Young quartz tubes under an atmosphere of purified dinitrogen. Solid state EPR spectra were recorded in the temperature range of 6 - 290 K on a JEOL continuous wave spectrometer JESFA200 equipped with an X-band Gunn diode oscillator bridge, a cylindrical mode cavity, and a N_2/He cryostat. Experimental conditions: microwave frequency ν = 8.96 GHz, modulation width = 0.5 mT, microwave power = 0.01 mW, modulation frequency = 100 kHz, time constant = 0.1 s. Spectral simulation was performed using the program W95EPR written by F. Neese.[3]

1 http://www.chem.gla.ac.uk/~louis/software/platon/; A. L. Spek, *Acta Cryst.*, 2009, **D65**, 148-155.
2 G. A. Bain and J. F. Berry, *J. Chem. Educ.,* 2008, **85**, 532-536.
3 F. Neese, *Diploma thesis,* University of Konstanz (Konstanz, Germany), **1993.**

2. Characterisation

Thermal Properties of Me_4-ACTBA:

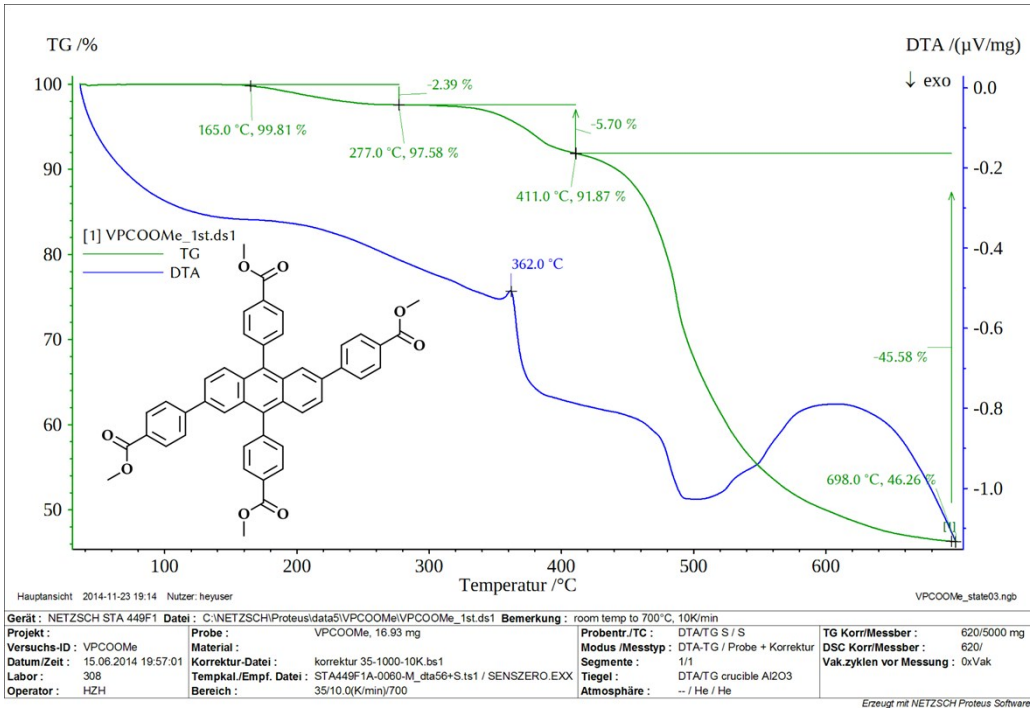

Thermal Properties of H_4-ACTBA:

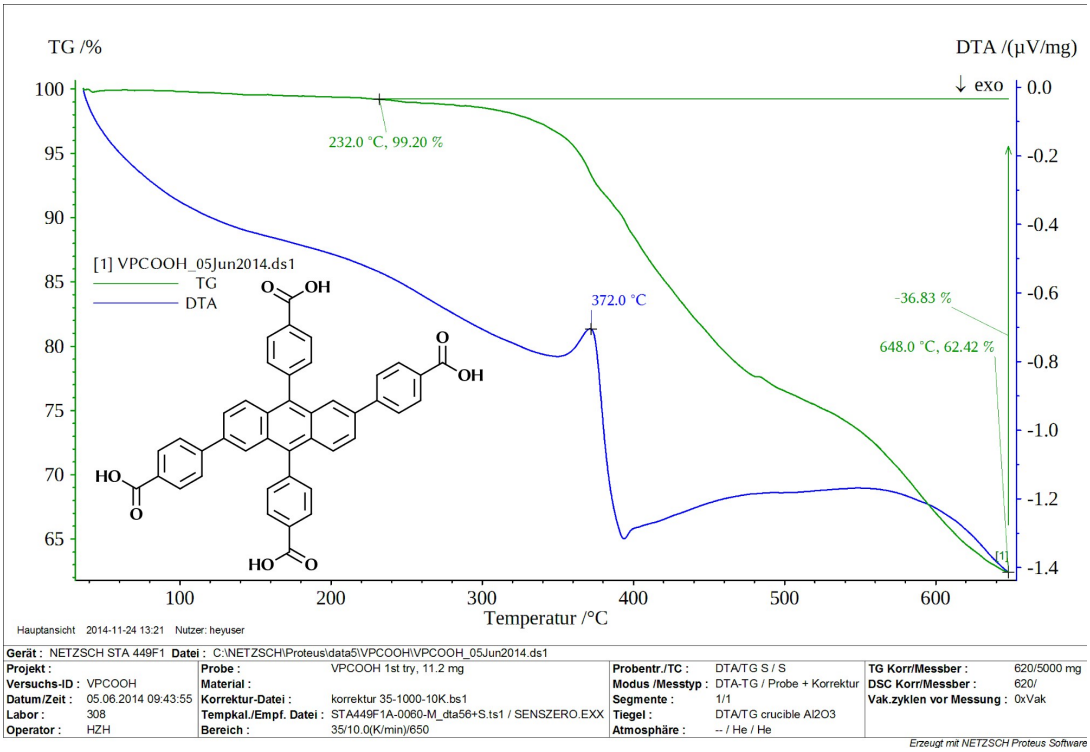

UV-Vis spectra

H_4-ACTBA in ^{i}PrOH:

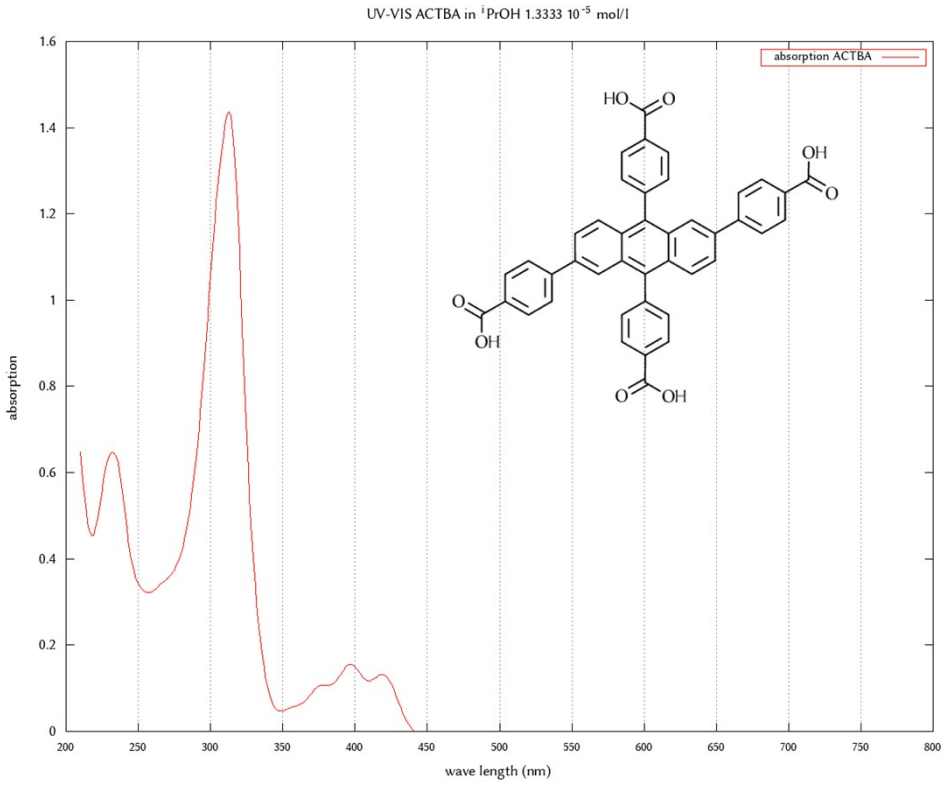

ACTBA in H_2O:

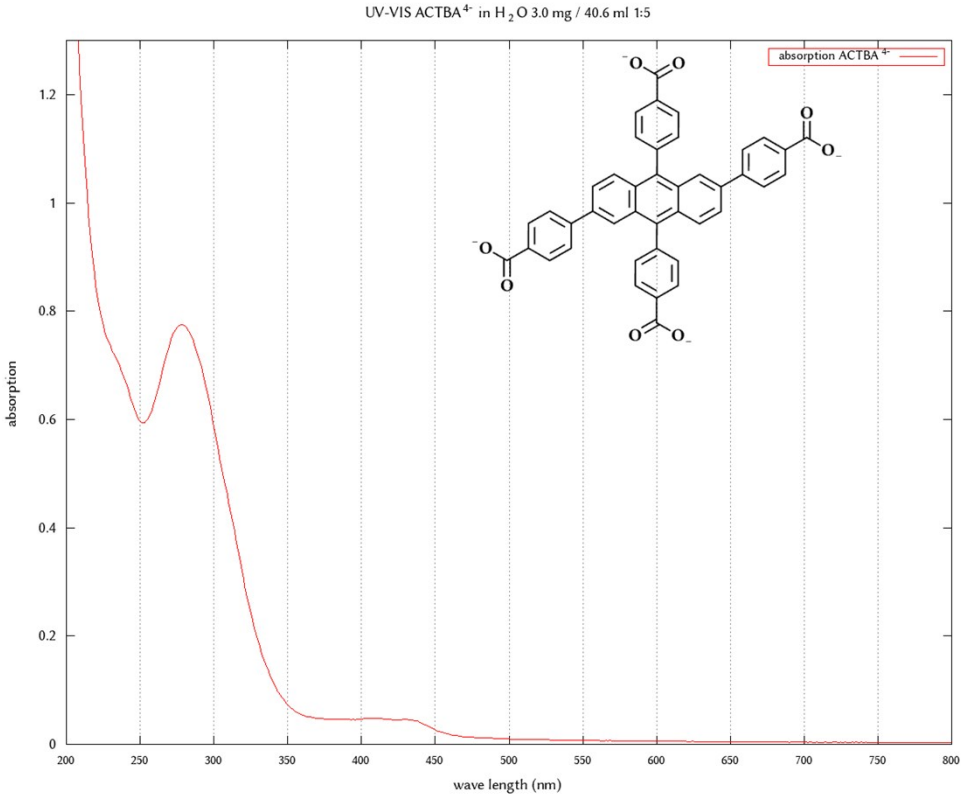

3. X-Ray Powder Diffraction Studies of 1

Prior to powder diffraction studies, **1** was treated at 200 °C under reduced pressure to evaporate volatile material (solvent molecules in pores). A comparison of obtained and simulated powder diffraction data is shown in Fig. S1.

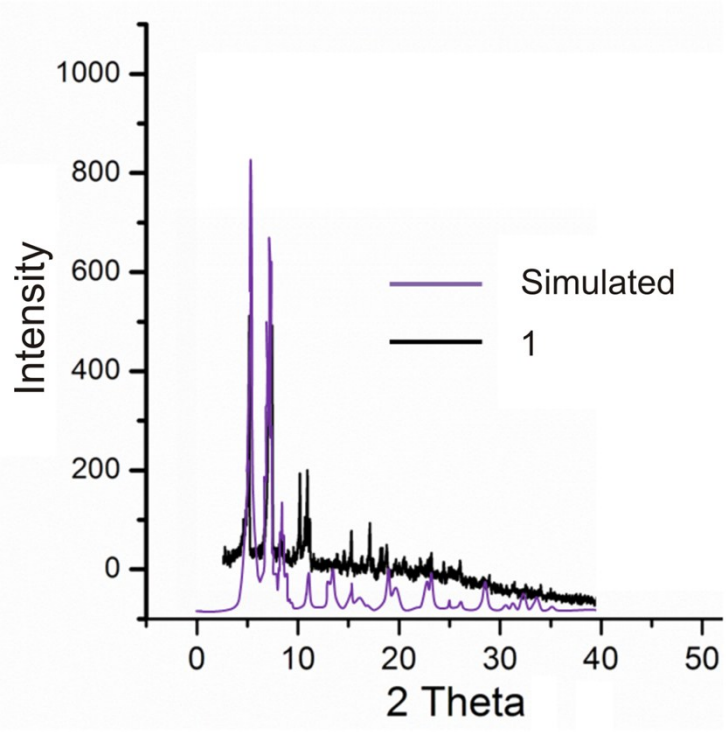

Fig. S1: Experimental (black) and simulated (purple) PXRD patterns of **1** (after heating to 200 °C for 120 min).

4. Surface Area of 1 and Pore Size Distribution

4.1. Surface Area of 1 (Quantachrome Nova 1200)

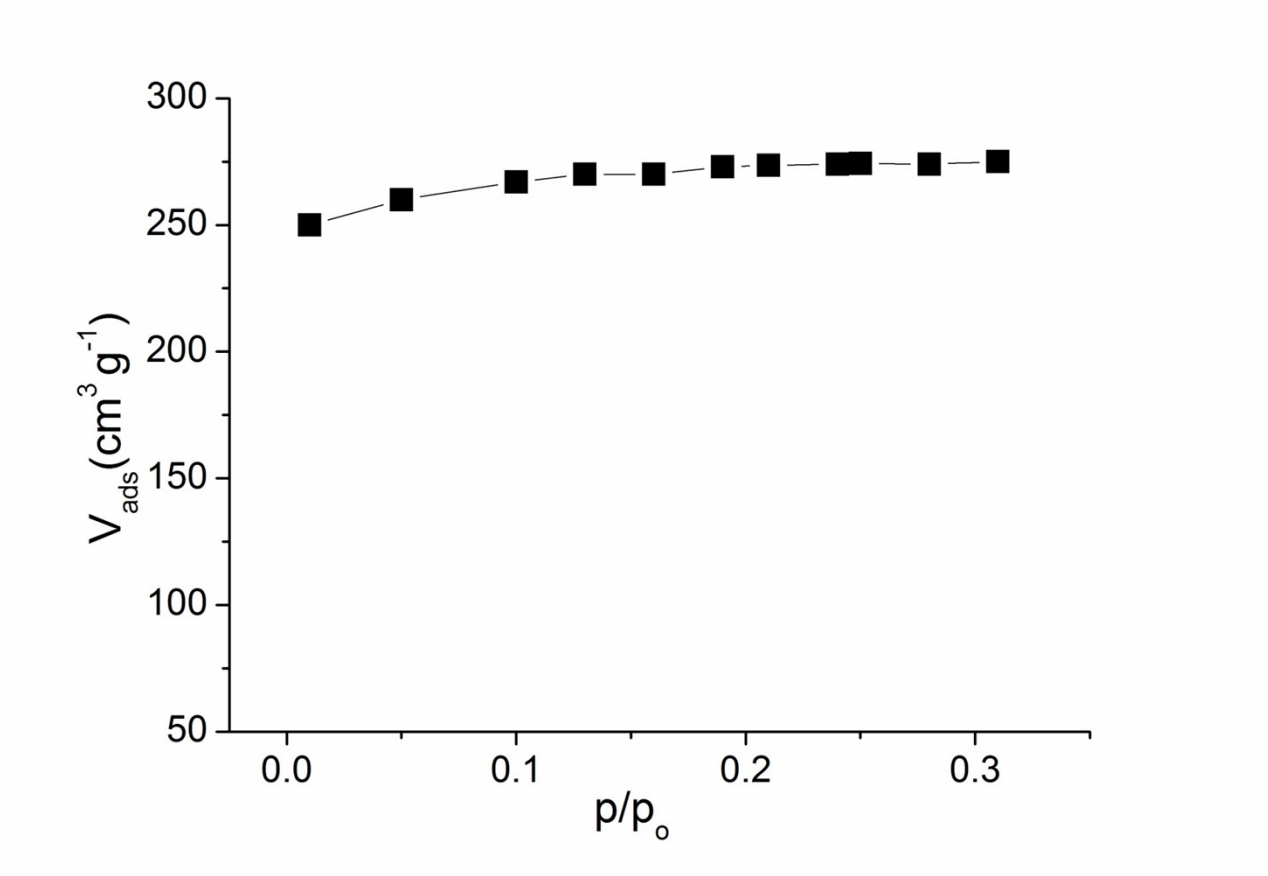

Fig. S2: Nitrogen sorption isotherm of **1** at T = –196 °C (p_o = 1 atm).

10 mg of **1** were activated under vacuum (10^{-3} torr) for 15 h at 200 °C. Specific surface area measurements have been performed using low-temperature nitrogen adsorption-desorption (Fig. S2). The data obtained correspond to a microporous state, as confirmed by the characteristic isotherm shape (type I).

Although N_2 at 77 K is considered a standard adsorbate when surface area and pore size are analysed, it is nevertheless universally recognised that nitrogen adsorption is unable to give satisfactory results for quantitative assessment of porosity, especially in the ultramicropore region with a width of less than 0.7 nm.

4.2. Micropore Size Distribution of 1

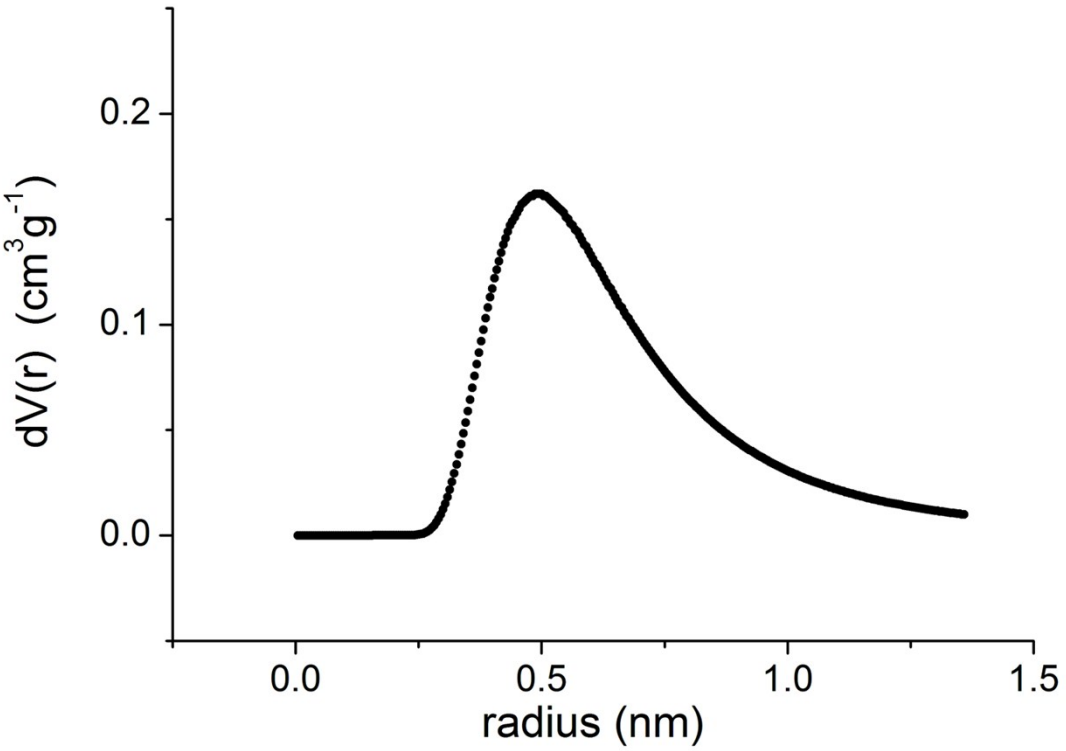

Fig. S3: Micropore size distribution calculated using the Dubinin–Astakhov (DA) method.[4]

The BET and Langmuir surface areas are 554 and 715 m^2g^{-1}, respectively, which are calculated using the adsorption data in the relative pressure range p/p_o = 0.06-0.3. The total pore volume of **1** is 0.164 cm^3/g; pore radius DA = 0.52 nm (Fig. S3).
The data obtained are in accord with the values of pore volume calculated using the program package Platon.[1] Thus, this parameter amounts to 0.1662 cm^3 at 298 K and 0.1635 cm^3 at 130 K.

4 M. M. Dubinin in "Progress in Surface and Membrane Science", eds. D. A. Cadenhead, J. E Danielli and M. D. Rosenberg, Academic Press, New York, 1975, no. 9.

5. Additional Pores in Directions 011, 101, 110 and 111 in 1

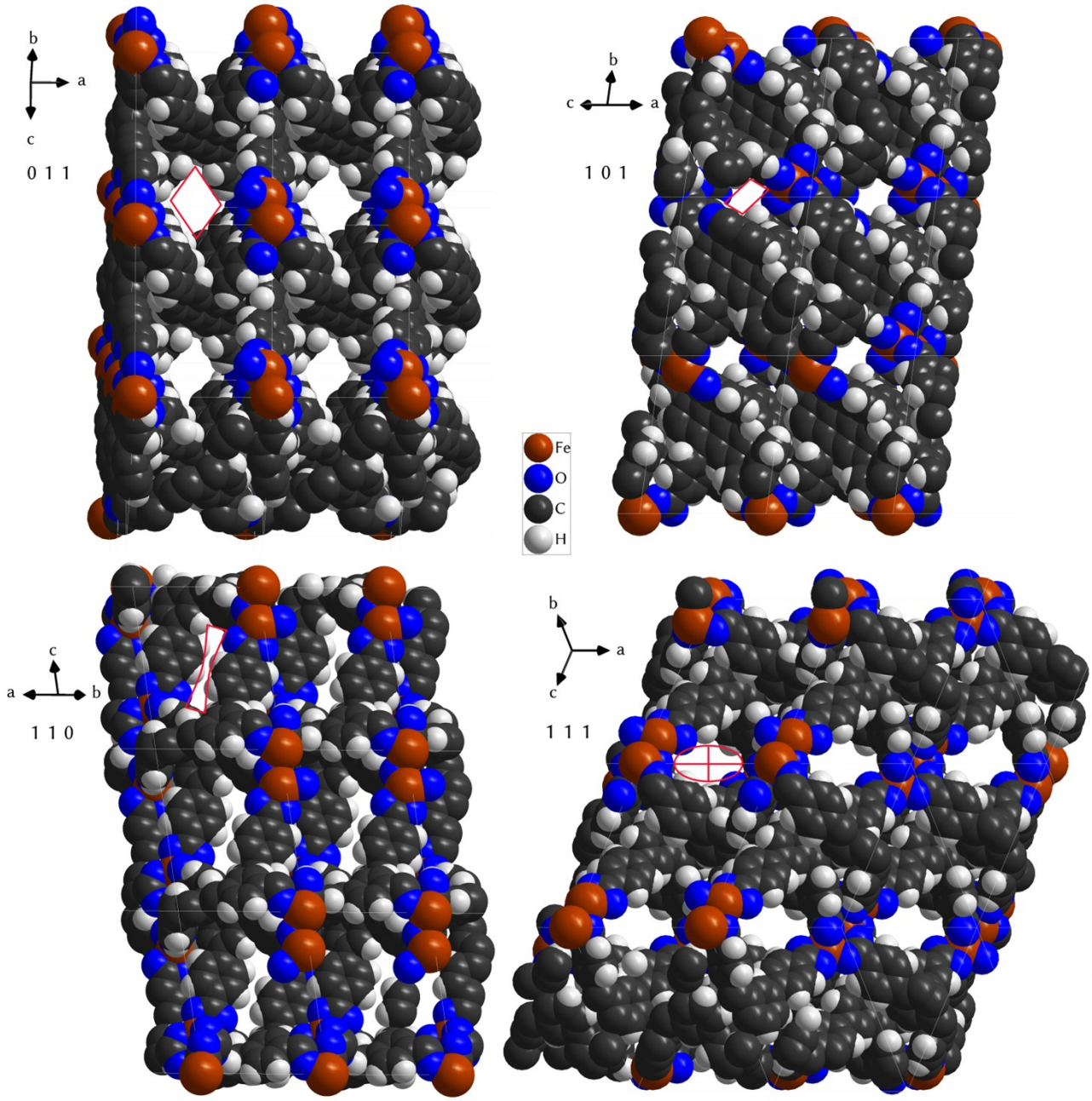

Fig. S4: Additional pores in **1**.

Approximate dimensions of the pores (see Fig. S4):
Pore 011 can be described by a parallelogram with dimensions of ca. 5.0 x 4.5 Å.
Pore 101 forms a tube that is still similar to a parallelogram of ca. 3.2 x 1.8 Å.
Pore 110 is a narrow slot of 7.5 Å with a concave inside ranging from ca. 1.5 to 0.5 Å.
Pore 111 can be illustrated by an elliptic shape with axes of ca. 6.3 x 3.5 Å.

6. Magnetic Susceptibility of 1

In order to understand the electronic structure of the trinuclear SBU in **1**, two independently synthesised, microcrystalline samples were tested for purity by elemental analyses and powder diffractometry, and studied by VT-SQUID, VT-X-band EPR, and zero-field ^{57}Fe Mößbauer spectroscopy at 77 K (see SI).

The SQUID magnetisation measurement (Fig. S5), recorded in a temperature range 2 – 300 K, revealed a reproducible, strongly temperature dependent magnetic moment over the entire temperature range. The magnetic moment at 2 K was determined to be 3.9 μ_B; thus, indicating an S_{tot} = 3/2 ground state for the SBU. With increasing temperature, the magnetic moment increases steadily to give a room temperature moment of approx. 11 μ_B, respectively. This implies an overall antiferromagnetic interaction.

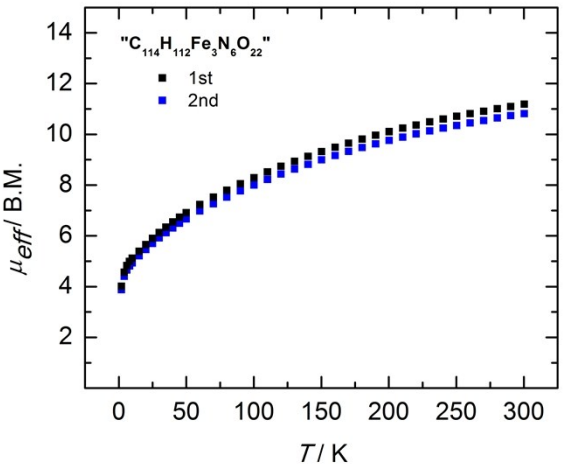

Fig. S5: SQUID magnetisation measurements of batch 1 of **1**.

We tried to analyse the temperature dependence of the magnetic susceptibility using the appropriate spin-Hamiltonian (eq. 1) for a linear trinuclear complex, which includes the isotropic Heisenberg-Dirac-van Vleck-exchange (HDvV), as well as the single-ion Zeeman interactions by using a full-matrix diagonalisation approach.

$$\hat{H} = 2\left(-2J_1\hat{S}_1\hat{S}_2\right) + \left(-2J_2\hat{S}_1\hat{S}_3\right) + \mu_B \sum_{i=1}^{3}(g\hat{S}_i\hat{B}) \qquad (1)$$

Scheme 1 illustrates the exchange coupling scheme used to model the susceptibility data for **1**. In this model, the exchange interaction between the neighbouring Fe ions is represented by J_1, whereas J_2 describes the interaction between the terminal Fe ions. The *g*-values were considered to be identical for the three Fe ions, and interactions between all three Fe ions were neglected. Modeling was performed with DAVE,[5] assuming three high-spin Fe^{III} (S = 5/2) ions (as suggested by the Mößbauer spectra). A system with two terminal high-spin Fe^{III} (S = 5/2) ions and a central Fe^{III} ion with intermediate spin (i.e. S = 3/2) was also considered. However, reasonable fits to the data could not be obtained in each case, even by considering the presence of a small amount of paramagnetic impurity (Fe^{III}, S = 5/2).

5 DAVE: A comprehensive software suite for the reduction, visualisation, and analysis of low energy neutron spectroscopic data, R.T. Azuah, L.R. Kneller, Y. Qiu, P.L.W. Tregenna-Piggott, C.M. Brown, J.R.D. Copley and R.M. Dimeo, *J. Res. Natl. Inst. Stan. Technol.,* 2009, **114**, 341.

The magnetic properties of some related carboxylato-bridged Fe^{III} complexes have been reported. A representative example is the complex $[Fe_2(OH)(\mu\text{-}OAc)_2(TMIP)](ClO_4)_2BF_4$, (TMIP = *tris*-(N-methylimidazol-2-yl)phosphine. In this complex, two Fe^{III} ions are antiferromagnetically coupled. J was found to be (-17 cm^{-1}).[6] Lippard has also reported a linear trinuclear Fe^{II} complex, $[Fe_3(O_2CPh)_6(BIPhOH)_2]$ (BIPhOH = bis(1-methyl-2-imidazolyl)phenylhydroxymethane) with a similar core structure to **1**. In this complex, competing ferromagnetic (J_1 = -2 ± 2 cm^{-1}) and antiferromagnetic exchange interactions (J_2 = 0.5 ± 0.5 cm^{-1}) were observed ($H = JS_iS_j$).[7]
J1 = -2+/-2 cm-1.

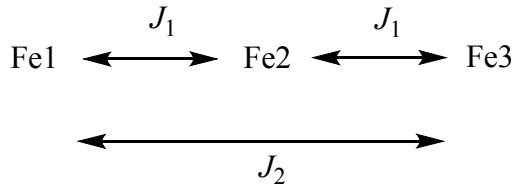

Scheme 1. Magnetic exchange pathways used for simulation of the magnetic susceptibility data for the trinuclear subunits in **1**.

7. Mößbauer Spectroscopy of 1

The zero-field Mößbauer spectrum of **1**, recorded at 77 K (Fig. S6), shows one symmetric quadrupole doublet with an isomer shift, δ, of 0.52 mms^{-1}, and a quadrupole splitting ΔE_Q of 0.70 mms^{-1}. These Mößbauer parameters are characteristic for high-spin Fe^{3+} (d^5, S =5/2) in an O-based ligand environment. However, a single Mößbauer feature appears to be inconclusive and not in agreement with the trinuclear SBU, as the Fe centers in **1** possess significantly different ligand environments. The outer Fe ions (Fe1, Fe1') are best described to be situated in a tetrahedral coordination sphere, while the central ion (Fe2) is clearly octahedrally coordinated (see main text). Accordingly, one would expect two Mößbauer signals with an intensity ratio of 2:1. In principle, both Fe sites (if high-spin S = 5/2) could possess similar Mößbauer parameters. With that said, the observation of a relatively sharp (Γ_{FWHM} = 0.57 mms^{-1}) and symmetric doublet still would not be anticipated. In addition, the formulation of three, magnetically coupled high-spin Fe ions cannot result in an electronic ground state S_{tot} of 3/2, as suggested by SQUID magnetisation.
An EPR spectroscopic study remains equally inconclusive. CW X-band EPR spectra of both batches, recorded at 8 and 6 K (Fig. S7), show very similar features with identical g-values. A signal at g = 8.47 and 4.13 is indicative for an S = 5/2 ion, for which the expected high-field third resonance is broadened into the baseline or hidden underneath the second, rhombic signal centred at g = 1.81, 2.00, and 2.18. Although these signals are remarkably reproducible, their intensities are not and, furthermore, are not in the expected integer ratio of 2:1 to each other. Accordingly, a temperature-dependent EPR study (6 to 290 K, Fig. S8) has been carried out. Clearly, with increasing temperature, the low-field feature at $g \approx 8.5$ and 4 loses signal intensity, while the resonance at $g \approx 2$ shifts to slightly lower fields, resulting in a single, broad resonance centered at g = 2.64, 1.97, and 1.90. It should be noted that the coalescence temperature is at around the 80 to 100 K, which could explain the single quadrupole doublet observed in the ^{57}Fe Mößbauer spectrum (recorded at 77 K).

6 F. J. Wu, D. M. Kurtz, Jr., K. S. Hagen, P. D. Nyman, P. G. Debrunner and V. A. Vankai, *Inorg. Chem.* **1990**, *29*, 5174-5183.
7 D. P. Goldberg, J. Telser, C. M. Bastos and S. J. Lippard, *Inorg. Chem*. **1995**, *34*, 3011-3024.

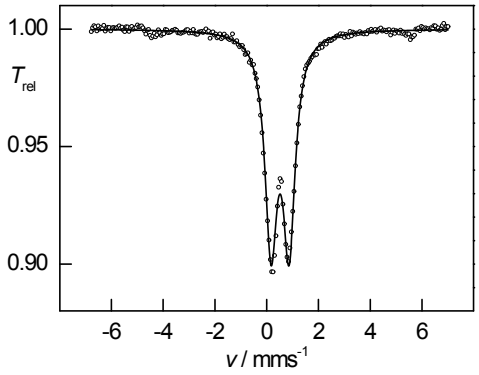

Type: doublet
Isomer shift δ = 0.52(1) mms^{-1}
Quadrupole splitting ΔE_Q = 0.70(1) mms^{-1}
Linewidth Γ_{FWHM} = 0.57(1) mms^{-1}

Fig. S6: Zero-field Mössbauer spectrum of batch 1 of **1**, recorded at 77 K.

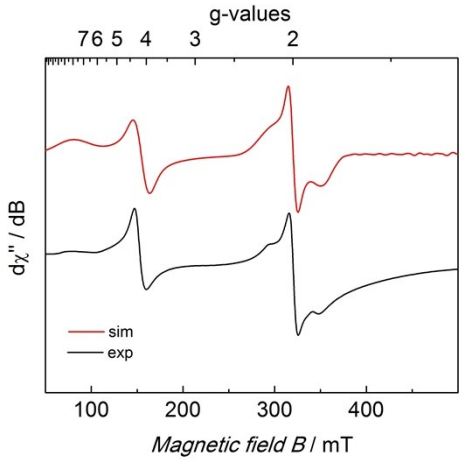

8 K:
Fe(III) S = 5/2, weight 1.00
g-values: g_x = 8.47; g_y = 4.13; g_z = 0.89
Linewidths: W_x = 20.6 mT; W_y = 8.26 mT; W_z = 4.27 mT

Fe(III) S = 1/2, weight 0.5
g-values: g_x = 1.81; g_y = 2.00; g_z = 2.18;
Linewidths: W_x = 12.0 mT; W_y = 4.2 mT; W_z = 17.1 mT

Fig. S7: X-Band EPR spectrum of batch 1 of **1**, solid state (recorded at 8 K).

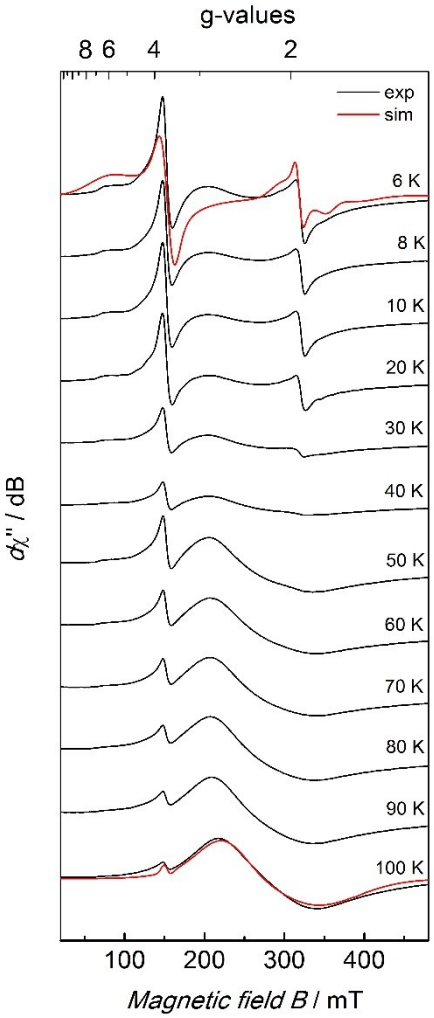

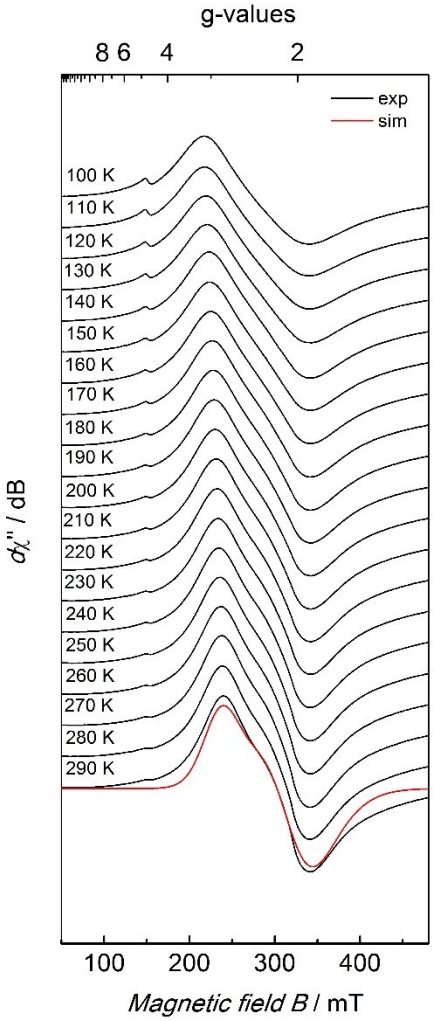

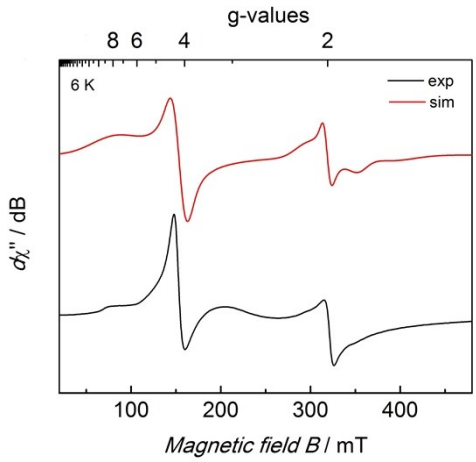

6 K:
Fe(III) S = 5/2, weight 1.00
g-values: g_x = 8.47; g_y = 4.13; g_z = 1.64
Linewidths: W_x = 30.0 mT; W_y = 8.26 mT; W_z = 30.0 mT

Fe(III) S = 1/2, weight 0.1
g-values: g_x = 1.81; g_y = 2.01; g_z = 2.18
Linewidths: W_x = 12.0 mT; W_y = 4.2 mT; W_z = 16.0 mT

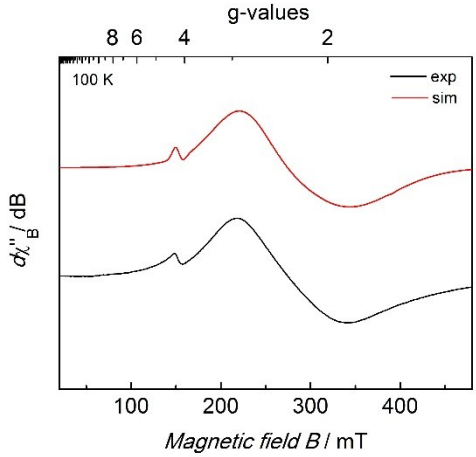

100 K:
Fe(III) S = 5/2, weight 0.0056
g-values: g_x = 4.22; g_y = 4.22; g_z = 1.635234
Linewidths: W_x = 5.0 mT; W_y = 5.0 mT; W_z = 4.0 mT

Fe(III) S = 1/2, weight 1
g-values: g_x = 2.68; g_y = 2.15; g_z = 1.98
Linewidths: W_x = 29.5 mT; W_y = 90.5 mT; W_z = 54.7 mT

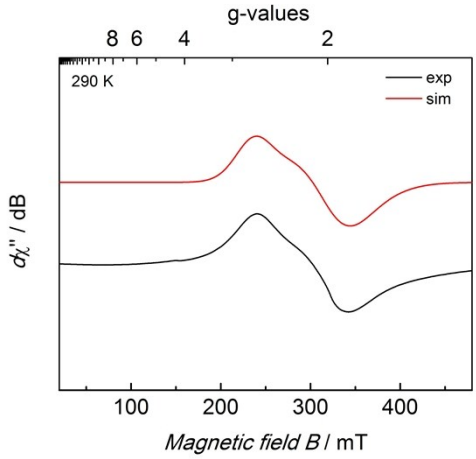

290 K

Fe(III) S = 1/2
g-values: g_x = 2.64; g_y = 1.97; g_z = 1.90
Linewidths: W_x = 218.1; W_y = 298.0; W_z = 569.9

Fig. S8: X-Band EPR spectroscopy of batch 2 of **1**, solid state (T-dependent EPR measurements).

8. Thermal Properties (DTA/TG) of 1

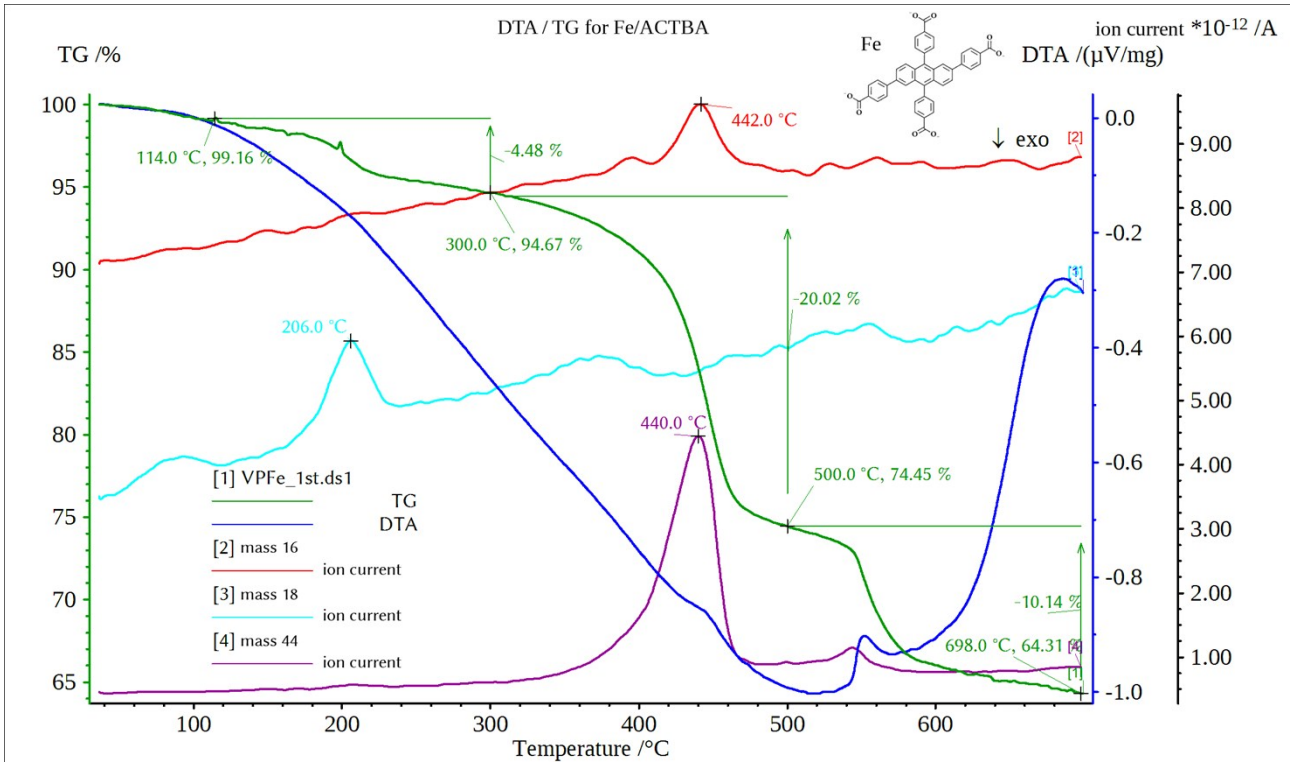

Fig. S9: DTA/TG analysis of **1** (green: TG, royal blue: DTA, red: 16 amu, turquoise: 18 amu (H_2O), violet: 44 amu (CO_2), heating rate 3 K / min, initial sample mass was 10.83 mg).

Compound **1** was isolated, washed with DEF, rinsed with MeOH and dried in air.
A bargraph scan up to 130 amu was taken. No presence of DEF or Et_2NH could be detected. From 114 °C to about 300 °C, roughly 4.5% weight loss is observed. The signal at 18 amu correlates to this step and indicates that water could be evaporated. Above 380 °C, rapid destruction occurs and a signal at 44 amu is observed (loss of CO_2, possibly from decarboxylation). In addition, a signal for 16 amu was also detected at this point but it is unclear which substance could create such a signal; CH_4 and O_{nasc} seem unlikely. Further weight loss was observed above 500 °C (Fig. S9).

9. Optical Properties of 1

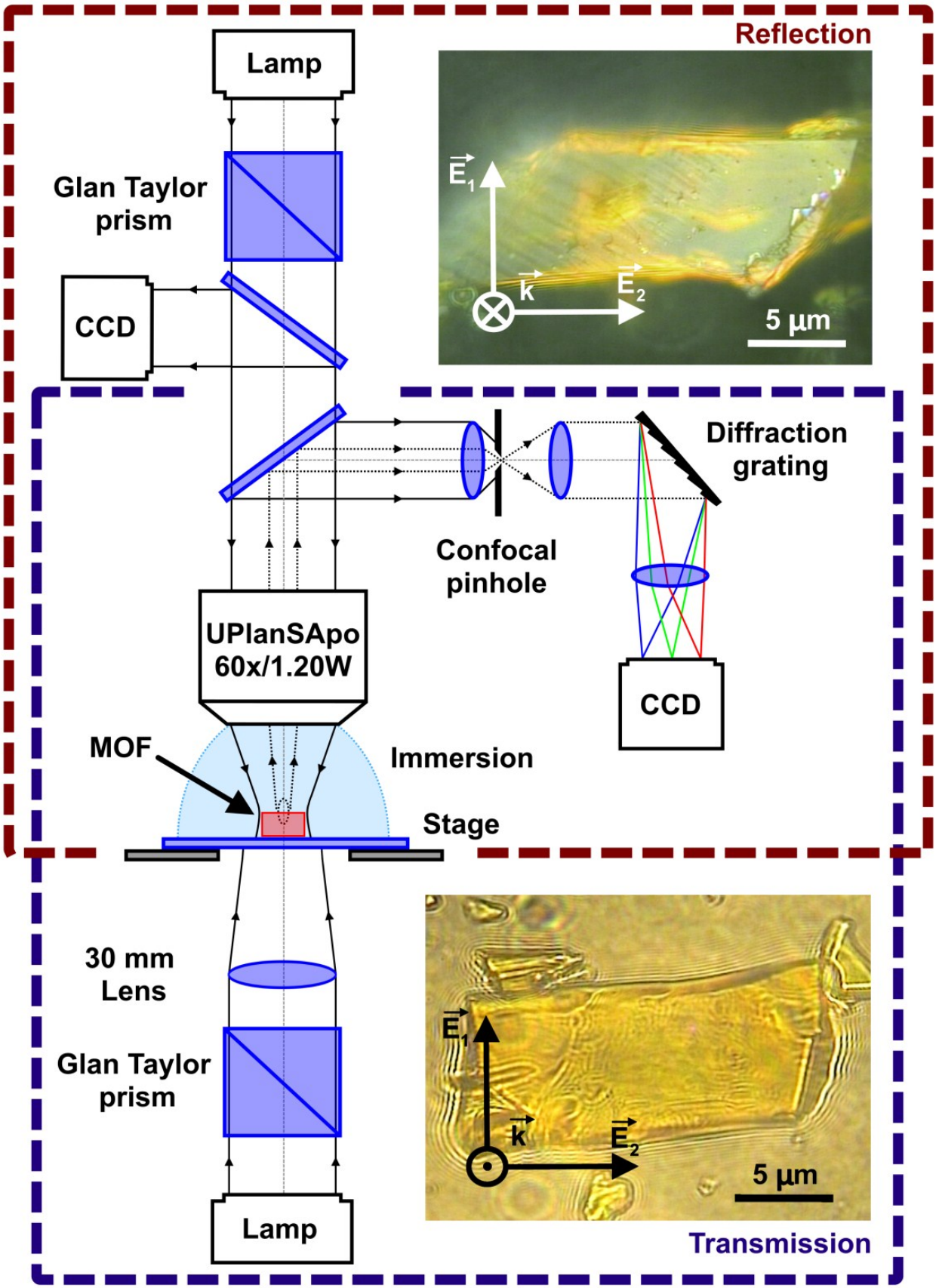

Fig. S10: Polarised transmittance and reflectance spectroscopy setup for single crystals of **1**. The upper and lower channels are for reflectance and transmission measurements, respectively.

A white light lamp was used as radiation source (Ocean Optics Halogen Light Source HL-2000-FHSA). Glan-Taylor prisms (ThorLabs SM1PM10) polarised this light in the channels of reflectance and transmission. Rotation of prisms in the optical system allowed transforming the electric vector of the electromagnetic waves from perpendicular (E1) or parallel (E2) with reference to the longest side of the crystal of **1**. Focusing of the polarised light and its collection from the single crystal's surface were carried out by an immersion objective (Olympus UPlanSApo 60x/1.20W) with a focus depth less than 1 μm. The single crystal was placed on an SiO_2 slide in DEF and irradiated by plane waves. The focusing of the polarised light in the reflectance channel was carried out by a 30 mm lens. Reflected or transmitted light was guided to a spectroscope with a 150 g/mm diffraction grating and a CCD (Andor DU420A-OE) with a working window from 200 to 1100 nm. Due to the pinhole onto which the light was focused, the spectroscope became a confocal one. This allowed measuring the spectra from an area as small as 4 x 3 μm.
The reflectance spectra were normalised by the spectra acquired under the same condition from a metallic mirror (ThorLabs PF10-03-F01) with known reflectance properties.

10. X-Ray Data for 1

Table S1. Crystal data and structure refinement of **1**.

Identification code	x1842sqfin	
Empirical formula	$C_{114}H_{110}ClFe_3N_6O_{22}$	
Moiety formula	$[\{Fe_3(C_{42}H_{22}O_8)_2\}Cl\cdot 6DEF]_n$	
Formula weight	2119.07	
Temperature	130(2) K	
Wavelength	0.71073 Å	
Crystal system	Triclinic	
Space group	$P\bar{1}$	
Unit cell dimensions	a = 13.3774(7) Å	α = 118.491(4)°
	b = 17.0481(7) Å	ß = 99.961(4)°
	c = 17.4322(7) Å	γ = 100.101(4)°
Volume	3285.1(3) $Å^3$	
Z	1	
Density (calculated)	1.071 Mg/m^3	
Absorption coefficient	0.407 mm^{-1}	
F(000)	1107	
Crystal size	0.2 x 0.15 x 0.05 mm^3	
Theta range for data collection	2.78 to 26.37°	
Index ranges	$-16 \le h \le 16$, $-21 \le k \le 21$, $-21 \le l \le 21$	
Reflections collected	55391	
Independent reflections	13416 [R(int) = 0.0674]	
Completeness to theta = 25.24°	99.8 %	
Absorption correction	Semi-empirical from equivalents	
Max. and min. transmission	1 and 0.98597	
Refinement method	Full-matrix least-squares on F^2	
Data / restraints / parameters	13416 / 0 / 466	
Goodness-of-fit on F^2	1.035	
Final R indices [I>2σ(I)]	R1 = 0.0541, wR2 = 0.1647	
R indices (all data)	R1 = 0.0817, wR2 = 0.1772	
Extinction coefficient	n/a	
Largest diff. peak and hole	0.618 and -0.605 $e\cdot Å^{-3}$	

Comments: Structure solution with SHELXS-2013 (direct method). Anisotropic refinement of all non-hydrogen atoms with SHELXL-2014.[8] All hydrogen atoms were calculated on idealised positions. Based on magnetic measurements the oxidation state of iron is +3 (Fe^{3+}). All attempts to locate highly disordered solvent molecules failed. The electron density for these highly disordered solvent molecules has been removed with the SQUEEZE routine implemented in PLATON.[1] From

8 SHELX includes SHELXS, SHELXL: G. M. Sheldrick, *Acta Cryst.,* 2008, **A64**, 112-122

the squeeze electron count we suggest to remove the electron density of 6 poorly defined and diffusely oriented DEF (diethylformamide) molecules from the unit cell and one chloride anion for charge neutrality reasons ((6 x 56) + (1 x 17) = 353 electrons). This value corresponds well with the estimated "squeezed" electron density of 344 electrons. A volume of 322 Å^3 for one DEF molecule (approximately 46 Å^3 for each non-hydrogen atom) is acceptable for extremely loosely packed and disordered solvent molecules.
The "squeezed volume" should normally not exceed the volume of 30% of the unit-cell. For this structure the solvent accessible volume of 1978 Å^3 represents 60 % of the unit cell. Although the program SQUEEZE is normally not designed to handle these extremely huge solvent areas, the result is convincing.

11. Ring Plane Angles

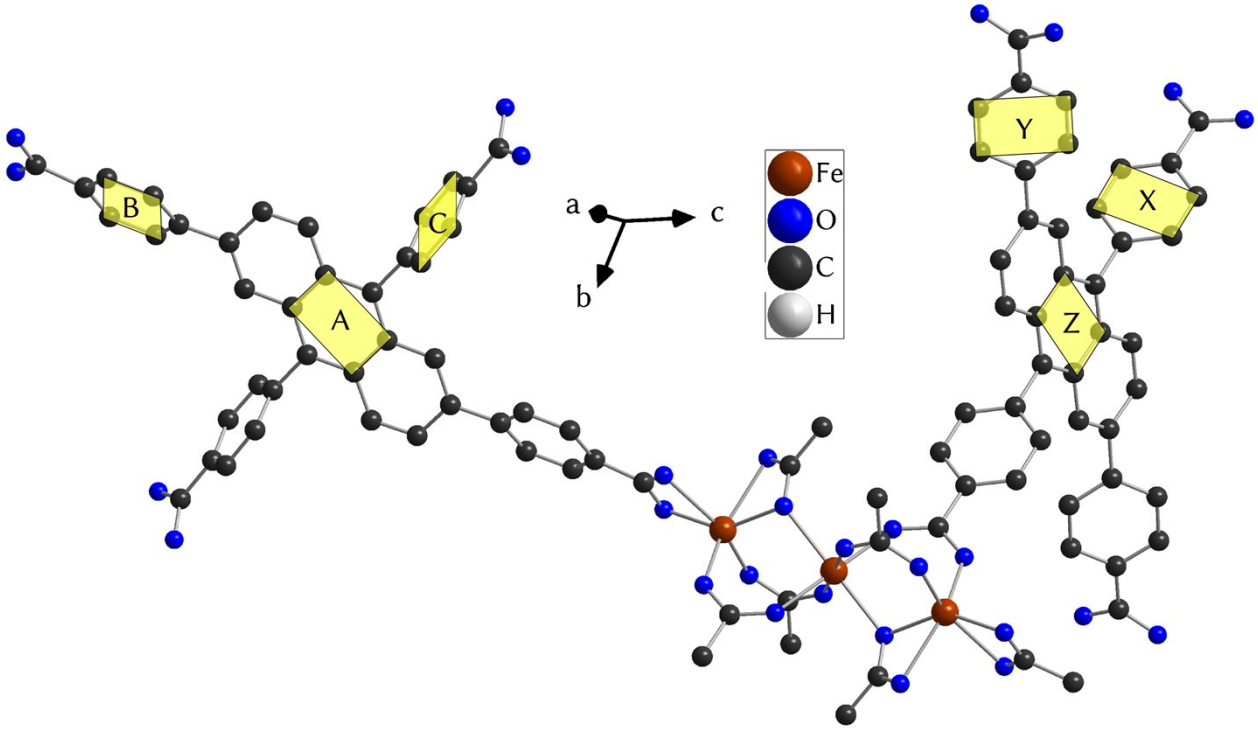

Fig. S11: Image showing various ring torsions / angles between planes.

There are two crystallographically different linker molecules present. The planar angles between the anthracene core (A, Z; central ring) and the surrounding phenylene groups (B, C and Y, X) are listed in Table 2. The planes A (through plane C9-C14-C9'-C14') and Z (C35-C30-C35'-C30') contain a centre of inversion.

Table S2. Angles between anthracene core (A, Z) and phenylene rings (B, C and Y, X) according to Fig. S11.

A		Z		A / Z angle
B	C	X	Y	
40.0°	67.5°	73.8°	45.5°	71.9°